Carbohydrate Polymers 103 (2014) 587–595

Contents lists available at ScienceDirect

Carbohydrate Polymers

journal homepage: www.elsevier.com/locate/carbpol

Controlled release of *Lactobacillus rhamnosus* biofilm probiotics from alginate-locust bean gum microcapsules

Wean Sin Cheow, Tie Yi Kiew, Kunn Hadinoto*

School of Chemical and Biomedical Engineering, Nanyang Technological University, Singapore 637459, Singapore

ARTICLE INFO

Article history:
Received 23 November 2013
Received in revised form
31 December 2013
Accepted 10 January 2014
Available online 21 January 2014

Keywords:
Functional food
Food microbiology
Nutraceuticals
Gut health
Probiotics capsules

ABSTRACT

Chitosan-coated alginate microcapsules containing high-density biofilm *Lactobacillus rhamnosus* have been previously shown to exhibit higher freeze drying- and thermal-tolerance than their planktonic counterparts. However, their cell release profile remains poor due to the capsules' susceptibility to the gastric environment. Herein the effects of adding locust bean (LB) and xanthan (XT) gums to alginate (AGN) capsules on the stress tolerance and cell release profiles in simulated gastrointestinal fluids are investigated. Compared to the AGN-only capsules, the AGN-LB capsules exhibit improved stress tolerance (i.e. ≈6× for freeze drying, 100× for thermotolerance, 10× for acid), whereas the AGN-XT capsules only improve the acid tolerance. Importantly, the AGN-LB capsules possess the optimal cell release profile with a majority of cells released in the simulated intestinal juice than in the gastric juice. The AGN-LB capsules' superiority is attributed to their stronger interaction with the chitosan coating and high swelling capacity, thus delaying their bulk dissolution.

1. Introduction

Probiotics, defined by the World Health Organization as "live microorganisms (bacteria or yeasts) which when administered in adequate amounts confer health benefits to the host" (WHO/FAO, 2002), have traditionally been viewed as food supplements. However, in recent years, probiotics have been increasingly prescribed as nutraceuticals in light of their therapeutic effects, which range from alleviating symptoms of lactose malabsorption and irritable bowel syndromes to suppressing colon cancer and enhancing resistance to gut infections (Kailasapathy & Chin, 2000; Sanders et al., 2013). The progress of probiotics from food supplements to nutraceuticals is best evidenced by the numerous (about 100) Phase III clinical trials currently ongoing, for treatment of atopic dermatitis, asthma, Crohn's disease, hepatic encephalopathy, rhinitis, and colorectal cancer, among others (Bethesda (MD): National Library of Medicine (US)). Significantly, about 70% of practicing consultant gastroenterologists in the United Kingdom prescribes probiotics to their patients to treat gastrointestinal disorders (Cordina, Shaikh, Shrestha, & Camilleri-Brennan, 2011), further demonstrating the emerging nutraceutical status of probiotics.

Probiotics confer their health benefits by inhibiting pathogen growths, maintaining health-promoting gut microflora, and stimulating the host's immune response (Figueroa-Gonzalez, Quijano, Ramirez, & Cruz-Guerrero, 2011). The probiotics must remain viable to confer these benefits, hence it hinges on their survival through the critical stages of processing and gastrointestinal transit. The form in which probiotics are usually prescribed as nutraceuticals – powders constituted of freeze dried probiotics with cryoprotectants, such as maltose (Cordina et al., 2011) – presents a hurdle over which the cells must overcome. Specifically, (i) the desiccation reduces viability and (ii) the absence of protective food matrix (such as yoghurt or cheese) exposes the probiotics to harsh gastrointestinal conditions after ingestion.

One effective method to protect probiotic cells from the stresses encountered during processing and gastrointestinal transit is by microencapsulation of probiotic cells into polysaccharide carrier matrices (e.g. alginate). Microencapsulation has been found to enhance the strain-dependent cell survival upon freeze drying (Heidebach, Forst, & Kulozik, 2010), as well as protect the cells from the acidic environment of the stomach and subsequently in facilitating the gradual cell release in the intestinal sections of the gut (Chavarri et al., 2010; Cook, Tzortzis, Charalampopoulos, & Khutoryanskiy, 2011; Guerin, Vuillemard, & Subirade, 2003; Kanmani et al., 2011). Although microencapsulation provides a physical protection barrier against external stresses, more can be

Abbreviations: AGN, alginate; AGN-LB, alginate-locust bean gum; AGN-XT, alginate-xanthan gum; CFU, colony forming unit; EPS, extracellular polymeric substance; HD, high density; LGG, *Lactobacillus rhamnosus GG*; MRS, de Man-Rogosa-Sharpe; PBS, phosphate buffer saline; SEM, scanning electron microscope; SGJ, simulated gastric juice; SIJ, simulated intestinal juice; SR, swelling ratio; SR_{max}, maximum swelling ratio; t_{max}, time at SR_{max}.

* Corresponding author. Tel.: +65 6514 8381; fax: +65 6794 7553.
E-mail addresses: wscheow@ntu.edu.sg (W.S. Cheow), tykiew@ntu.edu.sg (T.Y. Kiew), kunnong@ntu.edu.sg (K. Hadinoto).

0144-8617/$ – see front matter © 2014 Elsevier Ltd. All rights reserved.
http://dx.doi.org/10.1016/j.carbpol.2014.01.036

done to enhance the cells' innate robustness to further improve their viability. One such approach is to encapsulate probiotics in their biofilm form, a sessile high-density community of bacterial cells enclosed by a self-secreted extracellular polymeric substance (EPS), which is innately more robust than their planktonic counterparts. Biofilm cells have been found to exhibit greater resistance than planktonic cells to antibacterial agents (Cheow, Chang, & Hadinoto, 2010) and various stresses present in their environment (e.g. acid, heat) (Frank & Koffi, 1990; Zhu, Takenaka, Sato, & Hoshino, 2001), as a result of (i) their dormant metabolic state and quorum sensing ability, as well as (ii) the shielding presence of the EPS (Cheow et al., 2010). Importantly, the two most commonly used probiotics, *Lactobacillus* and *Bifidobacterium*, have been found to naturally exist in the gut in their biofilm states adhered to the gut lining (Macfarlane, Bahrami, & Macfarlane, 2011).

In view of their robustness, biofilm probiotics represent a better candidate for encapsulation as they are more tolerant upon exposures to stresses encountered during processing and gastrointestinal transit. Indeed, an earlier study comparing the encapsulation of planktonic and biofilm *Lactobacillus rhamnosus GG*, high-density biofilm cells encapsulated in chitosan-coated alginate capsules were shown to be superior in terms of the freeze drying viability and thermotolerance (Cheow & Hadinoto, 2013). Despite the superiority of the high-density biofilm cells in these two aspects, the survival of the encapsulated cells in simulated gastric juice remained low, where only ≈15% of the encapsulated cells survived the acidic condition, thus resulting in limited amount of cells available for release in the intestinal region. It is worth to mention that a similar low gastric juice viability (≈16%) was observed by other researcher when planktonic *Bifidobacterium breve* cells were encapsulated in chitosan-coated alginate microcapsules (Cook et al., 2011).

In this study, we prepare high-density biofilm probiotic microcapsules – HD capsules in short – having the desirable gastrointestinal release characteristics, i.e. capsules in which the biofilm cells are protected from the gastric juice and minimally released in the stomach, leading to their gradual and complete release only in the intestines. To this end, alginate, which is commonly used for encapsulation of live bacterial cells owed to their biocompatibility and low cost (Burgain, Gaiani, Linder, & Scher, 2011), is mixed with locust bean gum (LB) or xanthan gum (XT) to form the capsule matrices. LB and XT are natural polysaccharides extensively used in the food industry as emulsifiers, thickeners, or stabilizers (Dolz, Hernández, Delegido, Alfaro, & Muñoz, 2007). The high affinities of LB and XT for water molecules (Torres, Moreira, Chenlo, & Vázquez, 2012) increase the swelling of the capsule matrices from which the viscous gel layers formed by LB and XT in their hydrated swollen state (Darwiche, Bjorgell, & Almer, 2003) is expected to slow down the onset of capsules dissolution, resulting in a delayed release of the encapsulated cells only in the intestinal region.

In addition to investigating the gastrointestinal release characteristics, we also examine the effects of LB and XT addition on the HD capsule's stress tolerance upon freeze drying, heat treatment, and acid exposure in simulated gastric juice. Moreover, the freeze drying viability and thermotolerance are also examined relative to the planktonic capsules to ensure that the LB and XT addition does not negate the aforementioned superior characteristics of the HD capsules in these two aspects. The freeze drying is performed as a desiccation step in order to preserve the encapsulated cells in the dry form, while the thermal treatment is a performed as a measure of the stress tolerance of the capsules, e.g. during heat treatment of encapsulated cells as a sterilization procedure. *Lactobacillus rhamnosus GG* is employed as the probiotic model owed to its clinically proven health promoting effects (Doron, Snydman, & Gorbach, 2005) and its confirmed biofilm-forming ability in vitro (Lebeer, Verhoeven, Velez, Vanderleyden, & De Keersmaecker, 2007). The HD capsules containing the biofilm probiotic cells are prepared by in situ cultivation of the planktonic cells inside the confined space of the capsules, resulting in the growth of high-density biofilm colonies. The HD capsules are coated with chitosan to enhance their gastrointestinal stability and also to function as a thermal protective layer (Zorea, 2011).

2. Materials and methods

2.1. Materials

Lactobacillus rhamnosus GG (ATCC 53103) – LGG in short – is purchased from ATCC (USA). Alginic acid sodium salt (AGN) is purchased from Alfa Aesar (USA). LB, XT, low molecular weight chitosan (50–190 kDa), calcium chloride ($CaCl_2$), sodium chloride (NaCl), potassium chloride (KCl), hydrogen chloride (HCl), potassium hydroxide (KOH), and potassium phosphate monobasic (KH_2PO_4) are purchased from Sigma–Aldrich (USA). Phosphate buffered saline (PBS), de Man-Rogosa-Sharpe (MRS) broth, and bacto agar are purchased from BD Biosciences (USA).

2.2. Preparation and characterization of LGG microcapsules

Two types of LGG microcapsules, i.e. planktonic and HD microcapsules, are prepared using AGN-LB, AGN-XT, AGN-LB-XT, and AGN-only matrices. The planktonic LGG-loaded AGN-LB capsules are prepared by the external gelation method. Briefly, 75 μL of overnight suspension of planktonic LGG (OD_{600} = 2.0) is added to 15 mL of 2% (w/v) sterile AGN-LB solution at AGN:LB mass ratio of 3:1. The resultant cell suspension is atomized into 100 mL of sterile 0.1 M $CaCl_2$ solution in a glass evaporating dish using a two-fluid atomizer (B-290 Buchi, Switzerland) at air and feed flow rates of 140 L/h and 3 mL/min, respectively. LGG-loaded microcapsules are formed immediately as a result of the interaction between the AGN and Ca^{2+} to form calcium alginate gel.

The capsules are allowed to harden for 30 min at 4 °C after which they are recovered from the $CaCl_2$ solution by gravity sedimentation. Centrifugation to recover the capsules is not performed to avoid the collection of non-encapsulated cells. Next, the chitosan coating is performed by adding 45 mL of 0.4% (w/v) chitosan solution at pH 6 to the wet capsules. The resultant capsule suspension is incubated for 30 min under 150 RPM orbital shaking at ambient temperature. Lastly, the chitosan-coated AGN-LB capsules are washed with $CaCl_2$ solution to remove the excess chitosan followed by their recovery by sedimentation.

The amount of viable cells encapsulated in the capsules is quantified in log (CFU/mg) by sonicating 100 μL of the wet capsules in 1 mL PBS for 20 s in an ice bath, using a probe sonicator at 40% power (Vibracell VC 505, Sonics, USA), followed by enumeration of the viable cells by the drop plate method after 48 h incubation at 37 °C on MRS agar. The dry powder capsules are obtained by freeze drying, immediately after preparation, for 24 h (Alpha 1–2 LD Plus, Martin Christ, Germany). The morphology (e.g. size, shape) of the wet capsules is characterized using a light microscope (CKX41, Olympus, Japan), whereas the morphology of the dry capsules is characterized by scanning electron microscope (SEM) (JSM-6700F, JEOL, USA).

The HD capsules containing the biofilm LGG are prepared using a similar method as that for the planktonic LGG, with the following modifications: (1) a forty-fold dilution of the overnight planktonic LGG suspension and (2) an additional incubation step prior to the chitosan coating step. Specifically, the capsules containing the planktonic LGG are incubated for 18 h in MRS broth supplemented with 0.1 M $CaCl_2$ to allow the growth of encapsulated planktonic

cells into high-density biofilm cells. Subsequently, the capsules are recovered and characterized in the same manner as the capsules containing planktonic LGG. When XT is used as the additive instead of LB, identical preparation steps are employed with XT replacing LB, whereas the AGN-LB-XT capsules are prepared at a AGN:LB:XT mass ratio of 6:1:1 with a total solid concentration of 2% (w/v). The AGN capsules are also prepared at 2% (w/v) solid concentration.

2.3. Freeze drying viability and thermotolerance

To examine the freeze-drying viability, 20 mg of the freeze dried capsules (or 100 μL of the wet capsules for the control) are sonicated for 10 s in 1 mL PBS to disintegrate the capsule matrices resulting in the cell liberation. Afterwards, the viable log (CFU/mg) is enumerated using the same drop-plate method described above. The freeze-drying viability is characterized in terms of log (N/N_0), where N_0 and N here represent the viable CFUs in the capsules before and after freeze drying, respectively.

To determine the thermotolerance under dry heat treatment, 40 mg of the dry capsules are placed in 2 mL microtube which is then placed in an oven (FD 53, Binder, Germany) pre-heated at 80 °C, 90 °C, or 100 °C. After 45 min, 1 mL of PBS is immediately added to each of the microtube containing the capsules. The amount of surviving cells is determined by first sonicating the capsules in an ice bath for 20 s, followed by drop plating on MRS agar. Enumeration of the viable CFUs is performed after incubation for 48 h at 37 °C. The thermotolerance is characterized in terms of log (N/N_0), where N_0 and N here represent the viable CFUs in the capsules before and after exposure to high temperature, respectively. The cell viability results reported here and in the following sections are based on the average of three independent experiments, using different batches of capsules prepared on different days, with two replicates each.

2.4. Viability and cell release profiles in simulated gastrointestinal fluid

2.4.1. Viability of the encapsulated cells in simulated gastric juice

The simulated gastric juice (SGJ) is prepared by adjusting the pH of 0.2% (w/v) NaCl solution to pH ≈ 3 by the addition of 1.0 M HCl to simulate the non-fasted condition of the stomach (Cook et al., 2011). The viability of the encapsulated cells in SGJ is determined by immersing 30 mg of the dry capsules in SGJ at 37 °C for 1 h. The capsules are subsequently sonicated to liberate the cells, and the amount of surviving encapsulated cells is determined by drop plating on MRS agar.

As the SGJ viability is influenced by the degree of chitosan coating of the capsules (Cook et al., 2011), the extent of interaction between the capsule matrix solutions (i.e. AGN, AGN-LB, and AGN-XT) and chitosan is examined from the turbidity of the mixtures at different pH values, where higher turbidity values reflect stronger interactions. The cationic CS interacts with the oppositely charged AGN, AGN-LB, and AGN-XT by electrostatic interaction, forming insoluble polyelectrolyte complexes. A high degree of interaction results in the formation of a higher concentration of polyelectrolyte complexes, thus leading to a more turbid suspension. For the turbidity measurement, 1 mL of AGN solution at 1 mg/mL is first mixed with equivolume of 1 mg/mL chitosan solution. Subsequently, the pH of the mixture is adjusted to pH 2–6 (±0.1) by using 0.1 M HCl or 0.1 M KOH. The volume of HCl or KOH used is monitored, and the final volume of the mixture is made up to 3 mL by using 0.1 M KCl solution to ensure that a total of 1 mL of 0.1 M electrolyte is present in the mixture. The standardization of the electrolyte amount in the mixture is necessary as polymer electrostatic interaction is affected by ionic strengths (Leclercq, Boustta, & Vert, 2003).

The turbidity is measured in three replicates at 600 nm immediately after pH adjustment is performed, using a UV–vis spectrophotometer (UV-Mini 1240, Shimadzu, Japan). The measured turbidity is corrected by the turbidity of AGN solutions alone, where the above procedure is carried out with deionized water replacing the chitosan solution, to ensure that the results reported are due to interaction between capsule matrices and chitosan, rather than due to the capsule matrices alone. The same procedure is repeated for AGN-LB and AGN-XT, with these solutions replacing the AGN solution.

2.4.2. Cell release in simulated gastrointestinal fluid

The simulated intestinal juice (SIJ) used in the in vitro cell release experiments is prepared following the method of (Cook et al., 2011). The SIJ is prepared by dissolving 6.8 g of KH_2PO_4 in 750 mL of deionized water, followed by adjusting the pH to ≈7.2 with 0.2 M KOH and topping up the volume to 1 L. In the cell release experiment, 20 mg of the dry capsules are incubated in 5 mL SGJ in a shaking incubator at 150 rpm and 37 °C. After 0, 0.5, and 1 h exposure to the SGJ, 100 μL of the SGJ is collected (without any capsules) and the amount of viable cell released in the SGJ is determined by drop plating. Afterwards, all the SGJ is removed by careful pipetting to prevent any capsules from being collected.

Subsequently, 5 mL of SIJ is added to the capsules and the capsules are again incubated at 37 °C. The amount of cells released from the capsules into the SIJ is enumerated every half-hourly for 4 h, resulting in a total simulated gastrointestinal transit time of 5 h. After 5 h, the amount of cells remaining in the capsules (i.e. viable cells that are neither released in SGJ nor SIJ) is determined by sonicating the capsules for 20 s in an ice bath, followed by drop plating on MRS agar. It is worth noting that the 1 h and 4 h incubation time in SGJ and SIJ, respectively, mimic the typical stomach and intestinal transit time in healthy human adults (Graff, Brinch, & Madsen, 2001).

To investigate the effect of swelling capacity of the different capsule formulation on the cell release profiles, the swelling ratio (SR) of the capsules is determined by measuring the weight change of the capsules in the simulated gastrointestinal juices across time. SR is calculated as the ratio of the weight of the wet capsules to that of the dry capsules. Briefly, 20 mg of the dry capsules are added into a microtube containing 2 mL SGJ. At intervals of 10, 30, and 60 min, the SGJ is carefully removed to avoid removal of any capsules, and the weight of the capsules is then determined. Fresh SGJ is then added back into the microtube to allow the capsules to continue to swell. After 60 min, SIJ is added to the capsules instead, and the weight of the capsules is determined at half-hour intervals for 2 h, with fresh SIJ replaced in the microtube at each time interval. The SR values reported represent the average of three independent experiments. In addition, the light microscope images of the capsules in SGJ and SIJ are obtained by continuously monitoring the individual capsules on a covered glass slide.

3. Results and discussion

3.1. Effects of LB and XT addition on cell density of the HD capsules

The feasibility of growing high-density biofilm LGG colonies in AGN-LB, AGN-XT, and AGN-LB-XT capsules is investigated first and compared with the HD capsules of AGN, which were successfully prepared in (Cheow & Hadinoto, 2013). Fig. 1A presents the cell density of the wet capsules from the four different formulations. The cell densities of the AGN-LB and AGN-XT capsules are similar to that of the AGN capsules at 7.4–7.7 log (CFU/mg), denoting the feasibility of AGN-LB and AGN-XT in producing HD capsules. In contrast, capsules prepared from AGN-LB-XT contain 10× fewer cells at 6.4 log (CFU/mg).

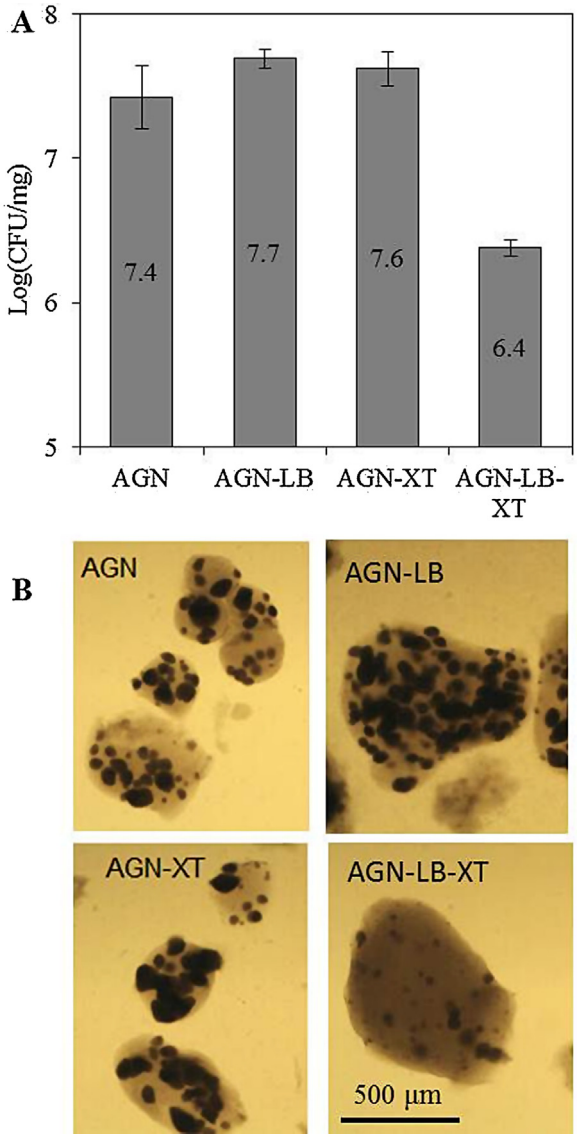

Fig. 1. (A) Encapsulation of biofilm LGG in AGN-LB and AGN-XT capsules results in comparable log (CFU/mg) as the AGN capsules; (B) light microscope images of the wet capsules indicate that fewer high-density colonies are present in AGN-LB-XT capsules – also reflected in the lower log (CFU/mg) in (A).

The light microscope images of the wet capsules in Fig. 1B, where the high-density biofilm colonies are reflected by the dark globules, also indicate the higher cell density of the AGN, AGN-LB, and AGN-XT capsules compared to that of the AGN-LB-XT capsules. The formation of rigid gels due to high synergy between LB and XT when mixed in the mass ratio of 1:1 (Copetti, Grassi, Lapasin, & Pricl, 1997) might be responsible for the lower cell growth due to space constraint. The average capsule size increases from 400 to 600 μm in the order of AGN < AGN-LB < AGN-XT < AGN-LB-XT. AGN-LB and AGN-XT capsules have larger sizes than AGN alone due to the higher affinity of the gums for water molecules (Torres et al., 2012). AGN-XT capsules are in turn larger than AGN-LB capsules due to the higher swelling capacity of the XT gum compared to the LB gum (Sujja-areevath, Munday, Cox, & Khan, 1998). On the other hand, AGN-LB-XT capsules are the largest as the high viscosity attributed to the interaction between LB and XT leads to bigger droplets being atomized, contributing to larger capsules. Considering the lower cell growth in AGN-LB-XT capsules, they are not investigated further.

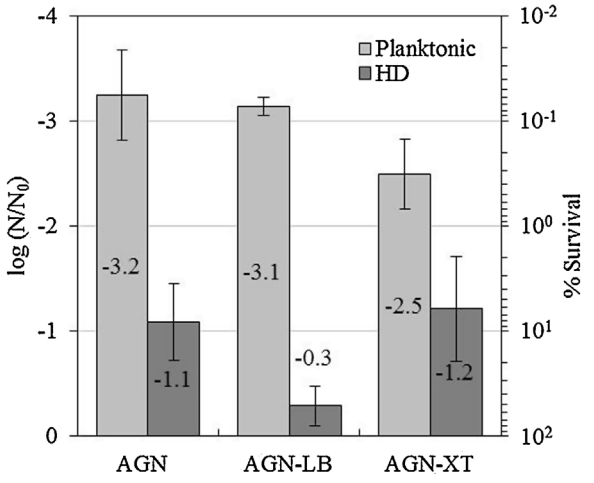

Fig. 2. Freeze drying viabilities of the planktonic versus HD capsules demonstrating the higher freeze drying tolerance of the HD capsules compared to their planktonic counterparts.

3.2. Stress tolerance of planktonic versus HD capsules

3.2.1. Freeze drying viability

Next, the HD capsules made of AGN, AGN-LB, and AGN-XT are compared to their planktonic counterparts in terms of their freeze drying viability and thermotolerance. Previously, the HD capsules have been found to be superior to their planktonic counterparts in terms of freeze drying viability for the AGN capsules (Cheow & Hadinoto, 2013). To test our hypothesis that the same can be observed even when AGN is supplemented with LB and XT, the capsules are freeze dried without external cryoprotectants (e.g. trehalose, sucrose), so that the role of the biofilm mode of growth in promoting the cell survival upon freeze drying can be isolated from that of the cryoprotectants.

Fig. 2 presents the freeze drying viabilities of the HD and planktonic capsules, where planktonic capsules clearly result in lower freeze drying viabilities with log (N/N_0) of −2.5 to −3.2, or a maximum of only 0.3% survival. Significantly higher freeze drying viabilities are observed for the HD capsules, with log (N/N_0) of −1.1 and −1.2 for the AGN and AGN-XT capsules, respectively, corresponding to ≈8% and ≈6% survival. Among the HD capsules, the AGN-LB capsules exhibit the highest freeze drying viability with 52% of the encapsulated cells surviving the freeze drying process, or a log (N/N_0) of −0.3. In terms of the degree of improvement in the freeze drying viability between the HD and planktonic capsules, the AGN-LB capsules result in the highest viability improvement. Specifically, the HD capsules of AGN-LB result in 660× viability improvements over their planktonic counterparts, compared to 125× and 20× for the AGN and AGN-XT capsules, respectively. The cryoprotectant action of LB can be attributed to its ability to retard formation of ice crystals during freezing (Kawahara et al., 2008).

While freeze drying affects the cell viability depending on the capsule matrices, the freeze dried capsules of AGN, AGN-LB, and AGN-XT are similar in size and shape as seen from the SEM images in Fig. 3A–C, owed to the same chitosan coating being used. The size of the dry capsules is relatively uniform at 400 ± 100 μm as shown in Fig. 3D using the AGN-LB capsules as the representative sample at a lower magnification. The CS coating on the capsules is present as a rough layer on the surface of all the capsules.

3.2.2. Thermotolerance

The thermotolerance results at 80 °C, 90 °C, and 100 °C are presented in Fig. 4A–C, respectively. At 80 °C, there is no appreciable difference between the planktonic and HD capsules of AGN,

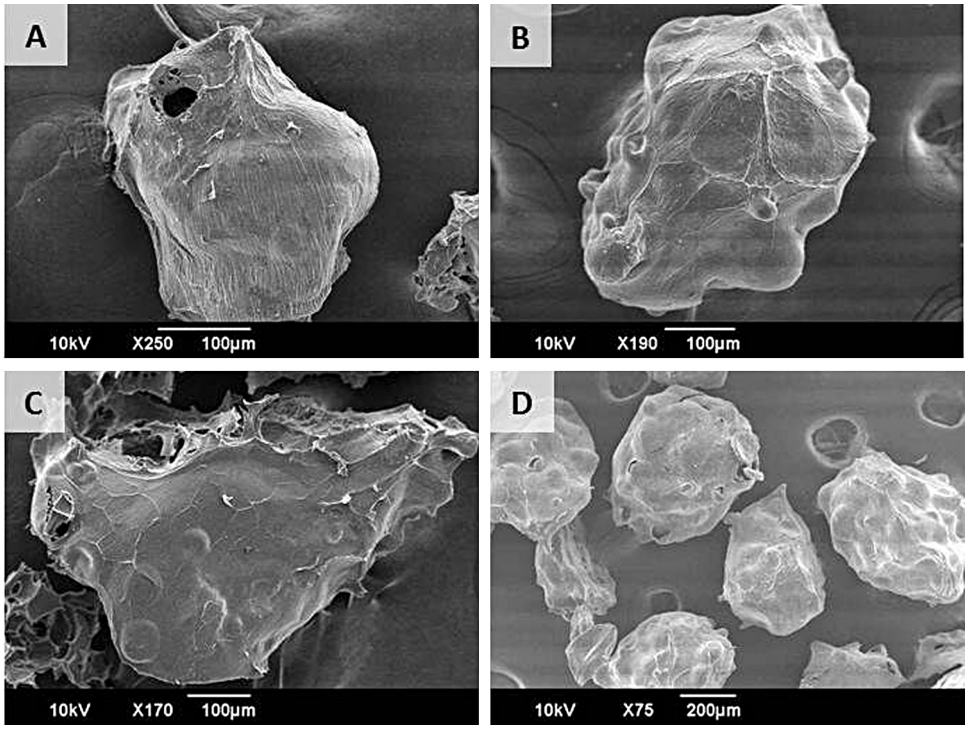

Fig. 3. SEM images showing chitosan-coated HD capsules of (A) AGN, (B) AGN-LB, and (C) AGN-XT, and (D) AGN-LB capsules are relatively uniform in size and shape.

AGN-LB, and AGN-XT. The AGN and AGN-LB capsules exhibit similar cell survival of 20–50% or log (N/N_0) of −0.3 to −0.6, while the AGN-XT capsules exhibit lower cell survival of 10–20% (log (N/N_0) ≈−0.8 to −1.0).

When the temperature is increased to 90 °C, the cell viability of the HD capsules remains indistinguishable from that of the planktonic capsules independent of the capsule formulation. All the capsules result in log (N/N_0) between −2.3 and −3.9, translating to <1% survival. Only upon increasing the temperature to 100 °C, a clear advantage of the HD capsules over the planktonic capsules can be observed for all the three capsules. Specifically, the planktonic capsules of AGN and AGN-LB results in no surviving cells (log (N/N_0) ≪ −1), while their HD counterparts results in log (N/N_0) of −5.9 and −3.3 for AGN and AGN-LB, respectively. The AGN-XT capsules demonstrate similar improvement, where the HD capsules exhibit higher thermotolerance at log (N/N_0) of −4.9 compared to −7.2 for the planktonic capsules, translating to a 200-fold increase in cell viability. Among the HD capsules, similar to the freeze drying viability, the AGN-LB capsules exhibit the highest thermotolerance among the three.

That the planktonic and HD capsules have similar thermotolerance at lower temperatures of 80 °C and 90 °C is not unexpected, as our previous study has shown that a sufficiently harsh environment is required to demonstrate the superiority of the HD capsules over the planktonic capsules (Cheow & Hadinoto, 2013). In the present study, the exposure of the capsules to a temperature of 100 °C for 45 min provides such harsh condition. Considering both the freeze drying viability and the thermotolerance, the superiority of the HD capsules to the planktonic capsules in the face of adverse stress conditions is evidently not compromised by the addition of LB and XT to AGN. In fact, the LB addition enhances the freeze drying viability and thermotolerance in comparison to the AGN-only capsules.

3.3. Viability of the encapsulated cells in simulated gastric juice

The viability of the encapsulated cells in the HD capsules after 1 h SGJ exposure is investigated next to ensure that the encapsulated cells are sufficiently protected from the acidic condition found in the stomach. The percentage of the encapsulated cells that remain viable after 1 h SGJ exposure, hence available for release in the SIJ, is presented in Fig. 5A. The AGN-LB capsules provide the highest level of protection to the encapsulated cells, where 92% of the encapsulated cells survive the SGJ, followed by the AGN-XT capsules with 47% cell survival. The AGN capsules are much inferior with only 9% of the encapsulated cells remain viable following the SGJ exposure.

To elucidate the reason behind the higher SGJ viability of the AGN-LB capsules, the interaction between the chitosan coating and the different capsule matrices is investigated because the chitosan coating has been identified as the factor governing the viability of encapsulated cells in SGJ (Cook et al., 2011). Two factors influence the encapsulated cell viability in SGJ, namely the (i) extent of chitosan coating at pH 6 and (ii) physical integrity of the chitosan coating upon exposure to SGJ at pH 3. The turbidity results of the interactions between chitosan and the AGN, AGN-LB, and AGN-XT mixtures are presented in Fig. 5B.

At pH 6, the pH at which the capsule coating is performed, a higher degree of interaction between chitosan and AGN-LB is observed as reflected by the higher turbidity level (≈0.3 a.u.) than that observed with AGN and AGN-XT (≈0.2 a.u). A higher turbidity indicates a higher degree of electrostatic interaction between the oppositely charged matrix material and CS, as a result of polyelectrolyte complex formation (Cook et al., 2011). A similar trend is observed at pH 3 in SGJ, where chitosan interact more strongly with AGN-LB than with AGN and AGN-XT. The stronger interaction with chitosan is anticipated to lead to more extensive chitosan coating on the AGN-LB capsules, possibly thicker, than that on the AGN and AGN-XT capsules. For the same reason, the chitosan coating on the AGN-LB capsules is expected to maintain its physical integrity better at pH 3.

These two characteristics of the chitosan-coated AGN-LB capsules result in a lower exposure of the encapsulated cells to the low pH environment, which is manifested in the higher SGJ viability of the AGN-LB capsules compared to the AGN and AGN-XT

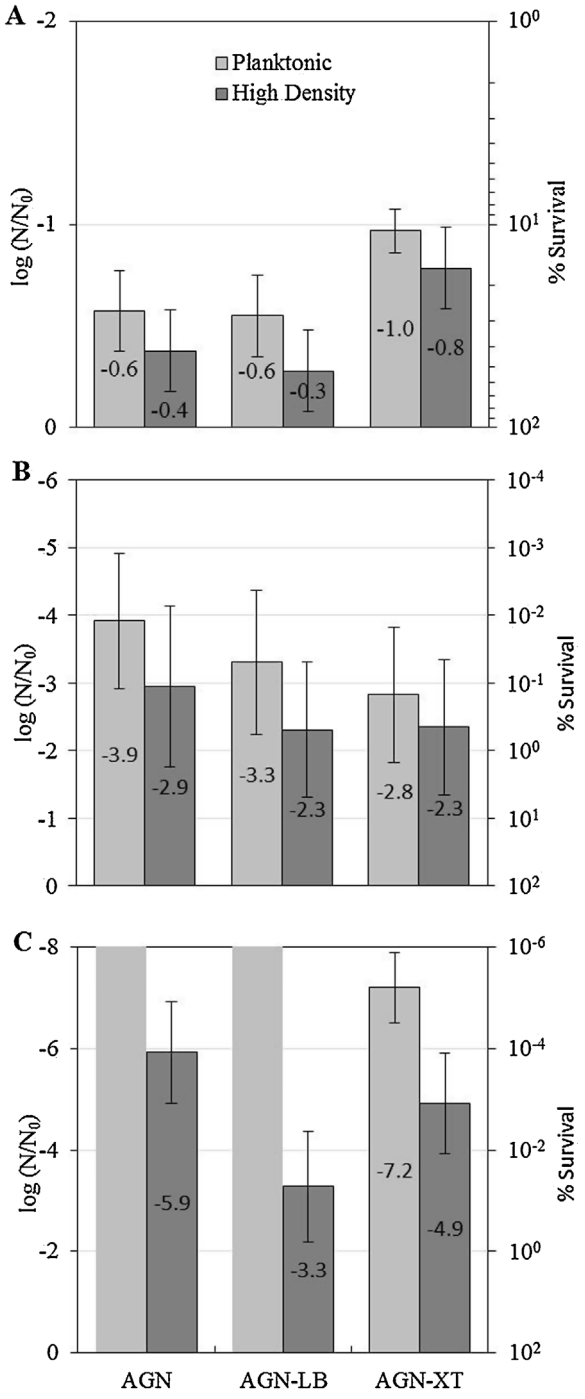

Fig. 4. Thermotolerance of planktonic and HD capsules upon exposure to temperatures of (A) 80 °C, (B) 90 °C, and (C) 100 °C for 45 min. The higher thermotolerance of the HD capsules is only evident at 100 °C.

capsules reported in Fig. 5A. Furthermore, the strength of interaction between chitosan and the capsule matrices in decreasing order is AGN-LB followed by AGN-XT, and lastly AGN. Hence, the turbidity results in Fig. 5B correspond nicely to the SGJ viability results in Fig. 5A, where the stronger the interaction between chitosan and the capsule matrices, the higher the acid tolerance of the capsules. On a side note, it is worth to mention that the stronger interaction with the chitosan coating in the AGN-LB capsules may also contribute to their aforementioned higher freeze drying viability and thermotolerance.

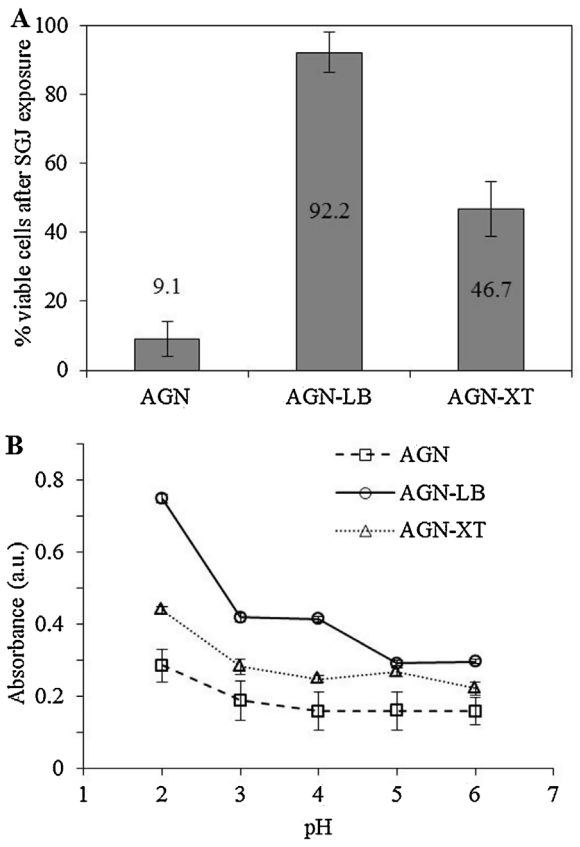

Fig. 5. (A) The percentage of the encapsulated cells that remains viable after 1 h exposure to SGJ at pH 3, with AGN-LB capsules demonstrating the highest SGJ survival, followed by AGN-XT and finally AGN capsules and (B) absorbance values from the turbidity tests at pH 2–6 demonstrating the stronger chitosan interaction with AGN-LB and AGN-XT compared to AGN across the pH range.

3.4. Cell release in simulated gastrointestinal fluid

The gastrointestinal release characteristics of the encapsulated cells from the HD capsules is investigated next, where the HD capsules are initially exposed to SGJ at pH 3 for 1 h after which the same capsules are transferred to SIJ at pH 7 for a further 4 h to mimic the gastrointestinal transit environment to which the capsules would be exposed upon ingestion. Fig. 6 presents the amount of viable

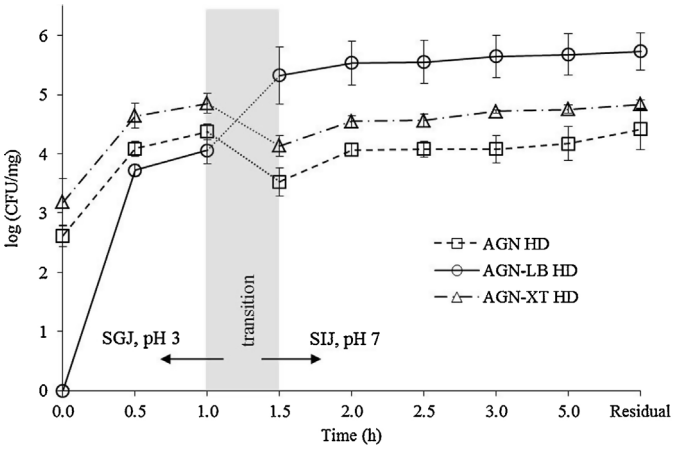

Fig. 6. Cell release profiles from the dry HD capsules of AGN, AGN-LB, and AGN-XT in simulated gastrointestinal fluid. The AGN-LB capsules possess the desired delayed release profile, where a larger number of the encapsulated cells are released in SIJ rather than in SGJ.

cells released from the HD capsules of AGN, AGN-LB, and AGN-XT across time, where the total amount of viable cells released after 5 h plus the amount of cells remaining in the capsules is presented as "Residual". The "Residual" values indicate that nearly all of the encapsulated cells are released from the capsules after 5 h for all the three capsules.

Upon exposure to SGJ, 2.6 and 3.1 log (CFU/mg) of cells are immediately released from the AGN and AGN-XT capsules, respectively. In contrast, no burst cell release is observed for the AGN-LB capsules. After 1 h incubation in the SGJ, the largest amount of cells released are from the AGN-XT capsules (4.9 log (CFU/mg)), followed by the AGN capsules at 4.4 log (CFU/mg), while the AGN-LB capsules release the smallest amount of cells in SGJ at 4.0 log (CFU/mg). The opposite is observed when the capsules are transferred to SIJ, where the AGN-LB capsules release the largest number of cells at ≈5.5 log (CFU/mg) across 4 h, which is significantly larger than a total of ≈4.2 and 4.7 log (CFU/mg) cells released by the AGN and AGN-XT capsules, respectively. The highest cell release rate displayed by AGN-LB capsules shows that the sizes of the capsules play a secondary role in the cell release rate, as the largest capsules with their corresponding lower surface area per unit volume available for dissolution is expected to result in slower dissolution, hence slower cell release rate.

To shed light on the cell release profiles of the capsules, further capsule characterizations are performed. The large number of cells immediately released in the SGJ for the AGN and AGN-XT capsules suggests that the cells populate the surface of the AGN and AGN-XT capsules. Indeed, SEM images of the capsule surfaces in Fig. 7 reveal the presence of a large number of cells on the surfaces of the AGN and AGN-XT capsules, while a relatively sparse cell population on the AGN-LB capsule surface is observed. In this regard, even though the cells on the surface are inadvertently exposed to the SGJ without any protection, these cells have minimal contribution to the lower SGJ viability of the AGN and AGN-XT capsules compared to that of the AGN-LB capsules discussed earlier. The reason is because Fig. 6 shows that the number of cells released from the surface constitutes less than 1% of the total amount of cells released indicating that a large majority of the cells are encapsulated.

The subsequent cell release profiles beyond the burst release are due to capsule dissolution, rather than diffusion through the pores in the capsule matrices, because of the small pore size (maximum of 200 nm) of the chitosan-coated AGN-based capsules (Cook et al., 2011). Therefore, the swelling ratio (SR) of the capsules, which are indicative of the capsules' physical integrity upon swelling, hence influencing the onset of capsule bulk dissolution, is examined. SR represents the net weight change of the capsules due to a combination of both swelling and dissolution in the SGJ and SIJ, where capsules with a high maximum SR (SR_{max}) can tolerate a high degree of swelling before their bulk dissolution takes place. The time at which SR_{max} is achieved, t_{max}, represents the time at which the SR starts to decrease sharply denoting the onset of bulk capsule dissolution.

Capsules with a later t_{max} are expected to result in the desired cell release profiles, where the capsules, including the chitosan coating, remain relatively intact in the SGJ, hence a minimal number of cells are released, followed by dissolution of the bulk of the capsules in the SIJ to release most of the encapsulated cells. Fig. 8A presents the SR of the AGN, AGN-LB, and AGN-XT capsules in the SGJ (time ≤ 1 h) and SIJ (time > 1 h). The AGN-LB and AGN-XT capsules display similar SR_{max} (≈18), whereas the SR_{max} of AGN is markedly lower at ≈8. The higher SR_{max} for the AGN-LB and AGN-XT capsules are expected by virtue of LB and XT's high water affinity characteristics (Torres et al., 2012).

Comparing the AGN-LB and AGN-XT capsules, the AGN-XT capsules dissolve at an earlier time as reflected in their t_{max} of 60 min compared to 90 min for the AGN-LB capsules. One of the factors that contribute to the lagged dissolution of the AGN-LB capsules is their aforementioned stronger interaction with the chitosan coating. The delay in the onset dissolution of the AGN-LB capsules results in fewer cells released in the SGJ compared to the AGN-XT capsules, which translates to the higher SGJ viability of the AGN-LB capsules as reported earlier in Fig. 5A.

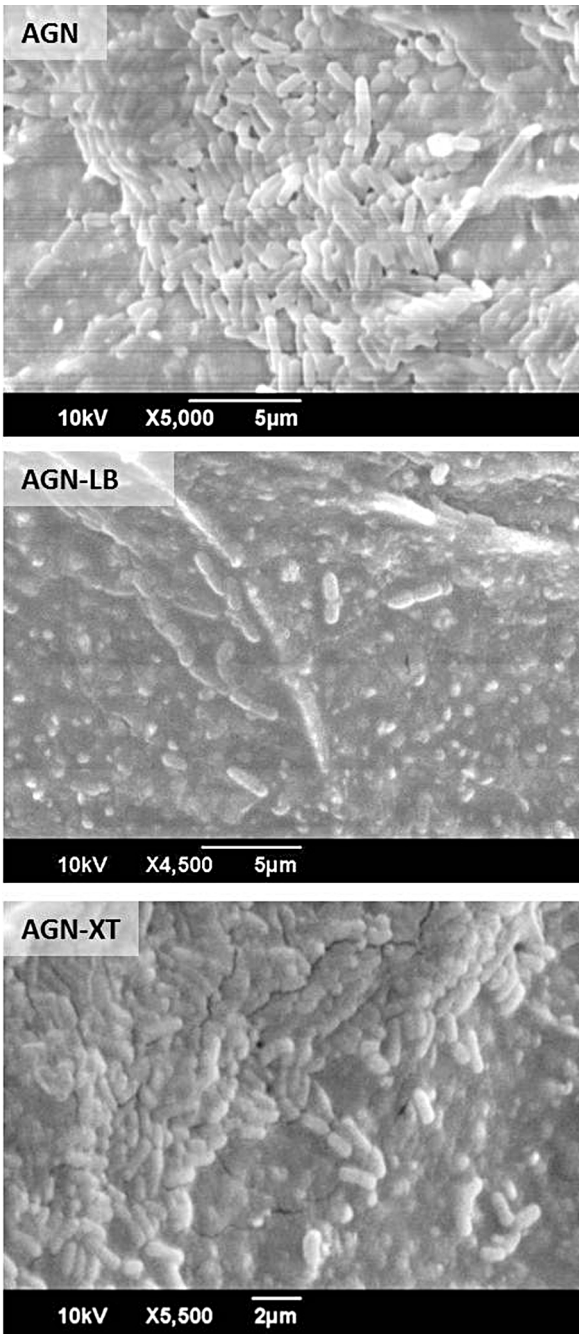

Fig. 7. SEM images showing higher cell densities on the surfaces of the AGN and AGN-XT capsules compared to the AGN-LB capsules.

For comparison between the AGN-LB and AGN capsules, the AGN capsules display a cell release profile markedly different from that of the AGN-LB capsules, despite both exhibiting the same t_{max}. It must be mentioned, however, that the dissolution behavior of the AGN capsules cannot be readily compared to that of the AGN-LB or AGN-XT capsules solely from their t_{max} due to their different SR_{max}. For this reason, transient light microscope images of the AGN and AGN-LB capsules upon their exposure to the SGJ and SIJ are

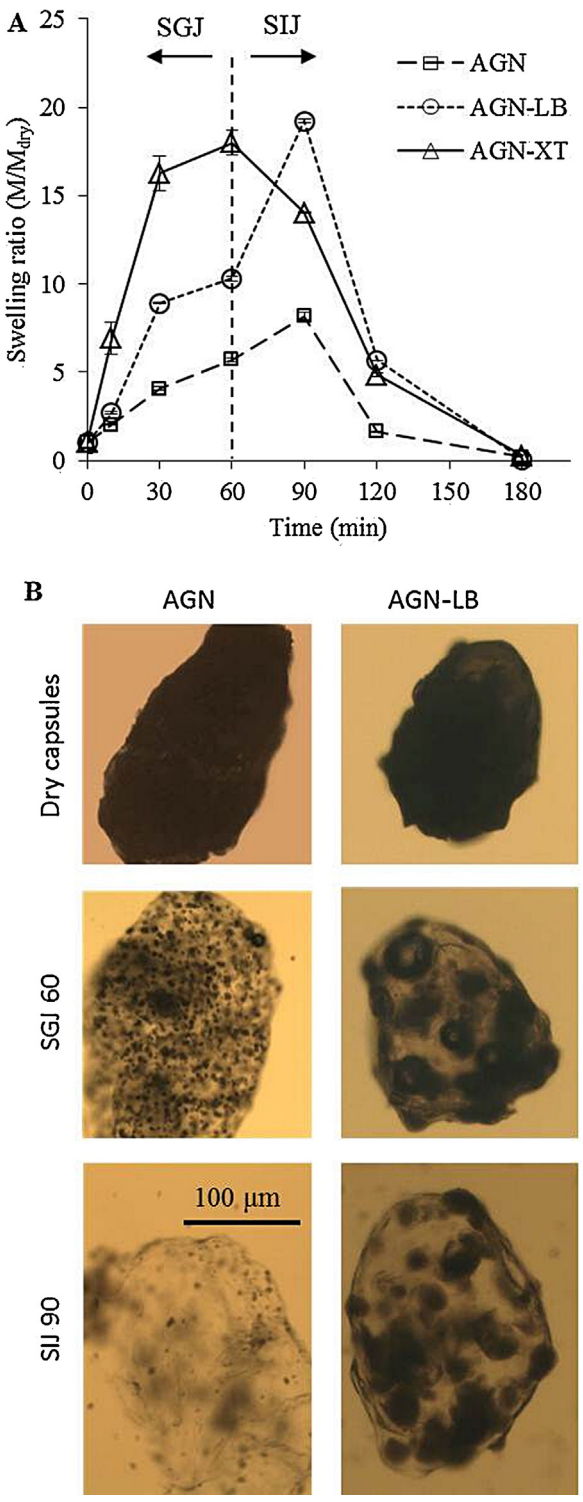

Fig. 8. (A) Swelling ratio profiles of the HD capsules explains the fewer cell released in the SGJ from the AGN-LB capsules compared to the AGN-XT capsules; (B) light microscope images of the AGN and AGN-LB capsules in simulated gastrointestinal fluids demonstrate the faster dissolution of the AGN capsules compared to the AGN-LB capsules. The scale bar of 100 μm applies to all images.

presented in Fig. 8B to elucidate the difference in their cell release profiles. At the start, the AGN and AGN-LB dry capsules are not distinguishable from the microscope images owed to their high density. After 60 min in the SGJ, both capsules increase in size relative to their respective dry capsules, where the size increase is more pronounced for the AGN capsules. When the capsules are transferred into SIJ, dissolution of the AGN capsules is apparent after 90 min, whereas the AGN-LB capsules continue to increase in size with much of the capsule remains relatively intact.

Relating the microscope images in Fig. 8B to the SR profiles in Fig. 8A for the AGN capsules, the larger size increase in the SGJ at 60 min compared to that of the AGN-LB capsules does not translate to a higher SR for the AGN capsules. Likewise, in the SIJ, the SR for the AGN capsules is at its maximum at 90 min although the microscope images suggest that dissolution of the capsules has clearly taken place. The discrepancy between the light microscope images and the SR profile for the AGN capsules, which is not observed for the AGN-LB capsules, suggest that dissolution of the AGN capsules occurs before the maximum swelling is achieved. The early onset of dissolution for the AGN capsules might be due to their aforementioned weak interaction with the chitosan coating. Indeed, when the swelling ratio experiment is performed with non-coated AGN capsules, complete dissolution is observed 60 min earlier compared to the coated AGN capsules (data not shown).

To summarize, the results support our hypothesis that the addition of LB to the AGN capsules improves the cell release characteristics, where a majority of the encapsulated cells are released in the SIJ. The presence of LB limits the burst release of cells from the capsule surface and the cells' acid exposure owed to the strong interaction between the chitosan and the AGN-LB matrices. When coupled with the high swelling capacity of the AGN-LB capsules, these result in the delay of the onset of capsule bulk dissolution into the SIJ. Significantly, the present study reaffirms the findings of (Cook et al., 2011), where the presence of CS coating on the surface of the AGN-LB capsules results in (1) delayed cell release with a majority of the cells released only in the SIJ, and (2) protection of the encapsulated cells from the low pH environment of the SGJ.

3.5. Overall comparison of the HD capsules

Having subjected the three different HD capsules to various stresses, the AGN-LB capsules are identified as the HD capsules having the best characteristics owed to their (i) highest freeze drying viability at 52% survival, (ii) highest thermotolerance when treated at 100 °C for 45 min, (iii) highest acid tolerance at 92% survival upon exposure to the SGJ, and (iv) desirable cell release profile in simulated gastrointestinal fluid, where a majority of the encapsulated cells are expected to be released in the intestinal region. On the other hand, there is no clear advantage of the AGN-XT capsules over the AGN capsules in terms of the freeze drying viability and thermotolerance. However, while both capsules exhibit relatively similar cell release profiles in the simulated gastrointestinal fluid, the higher acid tolerance of the AGN-XT capsules put them ahead of the AGN capsules.

4. Conclusion

The effects of incorporating LB and XT gums into the HD capsules of AGN coated with chitosan have been investigated in terms of (i) the capsules' stress tolerance upon freeze drying, heat treatment, and acid exposure in simulated gastric juice, and in terms of (ii) their cell release profiles in simulated gastrointestinal fluid. Similar to the AGN-only capsules, the HD capsules of AGN-LB and AGN-XT are superior to their planktonic counterparts in their freeze drying viability and thermotolerance, thus the addition of LB and XT gums does not negate the superiority of the HD capsules. Comparing the HD capsules, the AGN-LB capsules exhibit improved freeze drying viability (≈6×), thermotolerance at 100 °C and 45 min (≈100×), and acid tolerance (≈10×) compared to the AGN capsules. The same improvement is not achieved with the AGN-XT capsules, except for the improvement in the acid tolerance (≈5×). More importantly,

the AGN-LB capsules possess the optimal cell release profile in which a considerably larger number of cells are released in the simulated intestinal juice than in the gastric juice, unlike the AGN and AGN-XT capsules. The superior cell release characteristics of the AGN-LB capsules are attributed to their high swelling capacity and stronger interaction between chitosan coating and AGN-LB matrices, resulting in the delay of the onset of bulk capsule dissolution. The present results thus have demonstrated the importance of the capsule matrix material in the resultant cell release profile and acid tolerance, the future research direction is to investigate the effects of bacterial cell loading in the capsule on the same.

Acknowledgement

A financial support from the Ministry of Education of Singapore (Grant No. AcRF RG 76/10) is gratefully acknowledged.

References

Bethesda (MD): National Library of Medicine (US) ClinicalTrials.gov. Bethesda (MD): National Library of Medicine (US).

Burgain, J., Gaiani, C., Linder, M., & Scher, J. (2011). Encapsulation of probiotic living cells: From laboratory scale to industrial applications. *Journal of Food Engineering*, *104*(4), 467–483.

Chavarri, M., Maranon, I., Ares, R., Ibanez, F. C., Marzo, F., & Villaran, M. D. (2010). Microencapsulation of a probiotic and prebiotic in alginate-chitosan capsules improves survival in simulated gastro-intestinal conditions. *International Journal of Food Microbiology*, *142*(1-2), 185–189.

Cheow, W. S., Chang, M. W., & Hadinoto, K. (2010). Antibacterial efficacy of inhalable antibiotic-encapsulated biodegradable polymeric nanoparticles against *E. coli* biofilm cells. *Journal of Biomedical Nanotechnology*, *6*(4), 391–403.

Cheow, W. S., & Hadinoto, K. (2013). Biofilm-like *Lactobacillus rhamnosus* probiotics encapsulated in alginate and carrageenan microcapsules exhibiting enhanced thermotolerance and freeze-drying resistance. *Biomacromolecules*, *14*(9), 3214–3222.

Cook, M. T., Tzortzis, G., Charalampopoulos, D., & Khutoryanskiy, V. V. (2011). Production and evaluation of dry alginate-chitosan microcapsules as an enteric delivery vehicle for probiotic bacteria. *Biomacromolecules*, *12*(7), 2834–2840.

Copetti, G., Grassi, M., Lapasin, R., & Pricl, S. (1997). Synergistic gelation of xanthan gum with locust bean gum: A rheological investigation. *Glycoconjugate Journal*, *14*(8), 951–961.

Cordina, C., Shaikh, I., Shrestha, S., & Camilleri-Brennan, J. (2011). Probiotics in the management of gastrointestinal disease: Analysis of the attitudes and prescribing practices of gastroenterologists and surgeons. *Journal of Digestive Diseases*, *12*(6), 489–496.

Darwiche, G., Bjorgell, O., & Almer, L.-o. (2003). The addition of locust bean gum but not water delayed the gastric emptying rate of a nutrient semisolid meal in healthy subjects. *BMC Gastroenterology*, *3*(1), 12.

Dolz, M., Hernández, M. J., Delegido, J., Alfaro, M. C., & Muñoz, J. (2007). Influence of xanthan gum and locust bean gum upon flow and thixotropic behaviour of food emulsions containing modified starch. *Journal of Food Engineering*, *81*(1), 179–186.

Doron, S., Snydman, D. R., & Gorbach, S. L. (2005). Lactobacillus GG: Bacteriology and clinical applications. *Gastroenterology Clinics of North America*, *34*(3), 483–498.

Figueroa-Gonzalez, I., Quijano, G., Ramirez, G., & Cruz-Guerrero, A. (2011). Probiotics and prebiotics – Perspectives and challenges. *Journal of the Science of Food and Agriculture*, *91*(8), 1341–1348.

Frank, J. F., & Koffi, R. A. (1990). Surface-adherent growth of Listeria monocytogenes is associated with increased resistance to surfactant sanitizers and heat. *Journal of Food Protection*, *53*(7), 550–554.

Graff, J., Brinch, K., & Madsen, J. L. (2001). Gastrointestinal mean transit times in young and middle-aged healthy subjects. *Clinical Physiology*, *21*(2), 253–259.

Guerin, D., Vuillemard, J. C., & Subirade, M. (2003). Protection of bifidobacteria encapsulated in polysaccharide-protein gel beads against gastric juice and bile. *Journal of Food Protection*, *66*(11), 2076–2084.

Heidebach, T., Forst, P., & Kulozik, U. (2010). Influence of casein-based microencapsulation on freeze-drying and storage of probiotic cells. *Journal of Food Engineering*, *98*(3), 309–316.

Kailasapathy, K., & Chin, J. (2000). Survival and therapeutic potential of probiotic organisms with reference to *Lactobacillus acidophilus* and *Bifidobacterium* spp. *Immunology and Cell Biology*, *78*(1), 80–88.

Kanmani, P., Kumar, R. S., Yuvaraj, N., Paari, K. A., Pattukumar, V., & Arul, V. (2011). Cryopreservation and microencapsulation of a probiotic in alginate-chitosan capsules improves survival in simulated gastrointestinal conditions. *Biotechnology and Bioprocess Engineering*, *16*(6), 1106–1114.

Kawahara, H., Tokuno, Y., Sakamoto, M., Obata, H., Suzuki, M., Makishima, S., et al. (2008). Cryoprotective activity of shortened locust bean gum prepared by using food yeast *Candida utilis*. *Japan Journal of Food Engineering*, *9*(4), 289–296.

Lebeer, S., Verhoeven, T. L. A., Velez, M. P., Vanderleyden, J., & De Keersmaecker, S. C. J. (2007). Impact of environmental and genetic factors on biofilm formation by the probiotic strain *Lactobacillus rhamnosus GG*. *Applied and Environmental Microbiology*, *73*(21), 6768–6775.

Leclercq, L., Boustta, M., & Vert, M. (2003). A physico-chemical approach of polyanion-polycation interactions aimed at better understanding the in vivo behaviour of polyelectrolyte-based drug delivery and gene transfection. *Journal of Drug Targeting*, *11*(3), 129–138.

Macfarlane, S., Bahrami, B., & Macfarlane, G. T. (2011). Mucosal biofilm communities in the human intestinal tract. In A. I. Laskin, S. Sariaslani, & G. M. Gadd (Eds.), *Advances in applied microbiology* (Vol. 75) (pp. 111–143). San Diego: Elsevier Academic Press Inc.

Sanders, M. E., Guarner, F., Guerrant, R., Holt, P. R., Quigley, E. M., Sartor, R. B., et al. (2013). An update on the use and investigation of probiotics in health and disease. *Gut*, *62*(5), 787–796.

Sujja-areevath, J., Munday, D. L., Cox, P. J., & Khan, K. A. (1998). Relationship between swelling, erosion and drug release in hydrophillic natural gum mini-matrix formulations. *European Journal of Pharmaceutical Sciences*, *6*(3), 207–217.

Torres, M. D., Moreira, R., Chenlo, F., & Vázquez, M. J. (2012). Water adsorption isotherms of carboxymethyl cellulose, guar, locust bean, tragacanth and xanthan gums. *Carbohydrate Polymers*, *89*(2), 592–598.

WHO/FAO. (2002). *Guidelines for the evaluation of probiotics in food*. London: Author.

Zhu, M., Takenaka, S., Sato, M., & Hoshino, E. (2001). Influence of starvation and biofilm formation on acid resistance of *Streptococcus mutans*. *Oral Microbiology and Immunology*, *16*(1), 24–27.

Zorea, Y. (2011). Heat resistant probiotic compositions and healthy food comprising them. US Patent 0008493 A1.